

# Nonclassical Interference of Multimode Two-Photon Pairs with an Unbalanced Interferometer

Hayato Goto,<sup>1,2</sup> Haibo Wang,<sup>1</sup> Tomoyuki Horikiri,<sup>1,2</sup> Yasuo Yanagihara,<sup>1,2</sup> and Takayoshi Kobayashi<sup>1,2</sup>

<sup>1</sup>Core Research for Evolutional Science and Technology (CREST),  
Japan Science and Technology Corporation (JST)

<sup>2</sup>Department of Physics, Graduate School of Science,  
University of Tokyo, 7-3-1 Hongo, Bunkyo, Tokyo, 113-0033, Japan

(Dated: May 22, 2019)

Nonclassical interference of multimode two-photon pairs produced by an optical parametric oscillator (OPO) has been observed using an unbalanced interferometer. The time correlation between the multimode two photons has a multi-peaked structure. The use of the multimode two-photon state has enabled the observation of the nonclassical interference at nonzero delay time.

PACS numbers: 42.50.St, 42.50.Ar, 42.65.Lm

Quantum interference is one of the most interesting phenomena in quantum physics. Since the observation of nonclassical effects in the interference of two photons by Gersh and Mandel [1], several types of quantum interference experiments have been demonstrated using correlated two photons generated by spontaneous parametric down-conversion (SPDC) [2, 3, 4, 5, 6, 7, 8, 9]. In Refs. [1, 2, 3, 4, 5, 6, 7, 8, 9], higher visibility of two-photon interference than in the classical case is discussed as a typical nonclassical effect. Another feature of quantum interference has recently been studied since the proposal of quantum lithography by Boto et al. [10]. The feature is characterized by the phase dependence of two-photon interference. D'Angelo et al. have demonstrated quantum lithography for the first time using correlated two photons generated by SPDC, where the two narrower diffraction fringes than in the classical case was observed [11]. The nonclassical phase dependence of two-photon interference has also been confirmed using a conventional Mach-Zehnder interferometer [12].

In this Letter, we propose and demonstrate a new type of quantum interference experiment using multimode two-photon pairs produced by an optical parametric oscillator (OPO) [13, 14]. The experiment proposed here is shown in Fig. 1. The output beam from the OPO is incident at one of the input ports of an unbalanced interferometer. Before the discussion of the quantum feature of the experiment, let us consider the classical case when classical light of wavelength  $\lambda_0$  is incident to the interferometer instead of the OPO output. Let  $L = L_0 + L$  be the path-length difference of the interferometer, where  $L_0 = 1/\lambda_0$  (an integer) and  $0 < L < \lambda_0$ . The coincidence rate in the classical case is proportional to  $(1 + \cos \phi)^2$  with the phase difference  $\phi = 2\pi L/\lambda_0$ . The fringe period in this case is  $2\pi/\phi$ . In contrast, the period is expected to be  $\lambda_0$  as derived below when the multimode two-photon pairs are incident to the interferometer. Moreover, the nonclassical interference can also be observed at nonzero delay time, which has not been reported before. The observation can be explained in

terms of the property of the multimode two-photon state produced by the OPO as follows.

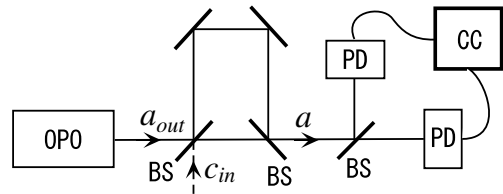


FIG. 1: Block diagram of the experiment to observe nonclassical interference of multimode two-photon pairs using an unbalanced interferometer. BS:50/50 beam splitter; PD: photodiode; CC: coincidence counter.

The output operator,  $a(t)$ , from one of the output ports of the interferometer is expressed as

$$a(t) = \frac{a_{out}(t - T_S) + c_{in}(t - T_S)}{2} + \frac{c_{in}(t - T_L) - a_{out}(t - T_L)}{2} \quad (1)$$

Here  $a(t)$  denotes a Fourier transform of a field operator,  $a(\omega)$ , of frequency  $\omega_0 + \Delta$  ( $\omega_0$  is the degenerate frequency of the OPO). That is, it is defined as

$$a(t) = \frac{1}{2\pi} \int d\omega a(\omega) e^{-i(\omega_0 + \Delta)\omega} \quad (2)$$

$a_{out}$  is the output operator of the OPO far below threshold [13].  $c_{in}$  is an annihilation operator of the vacuum entering the interferometer from the other of the input ports.  $cT_S$  and  $cT_L$  are the short and long path lengths of the interferometer, respectively ( $c$ : the speed of light in the vacuum). The intensity correlation function is derived as

$$\begin{aligned} I(\tau) &= \langle a^\dagger(t) a^\dagger(t + \tau) a(t + \tau) a(t) \rangle \\ &= \frac{p}{2} \frac{1}{\omega_0(\tau)} \cos \left( \frac{2\pi}{\lambda_0} \tau \right) + \frac{p}{\omega_0(\tau - T)} + \frac{p}{\omega_0(\tau + T)} \quad (3) \end{aligned}$$

Here we have dropped the higher-order term  $s$  than the square of the absolute value of the single-pass parametric amplitude gain  $j^2$ ;  $\langle \rangle$  is the intensity correlation function of the output from the OPO;  $T = T_L - T_S = L/c$  is the propagation time difference between the short and long paths in the interferometer.  $\langle \rangle$  is a multi-peaked function of  $\tau$  expressed as follows [13, 14]:

$$\langle \rangle = j^2 \frac{F^2}{F_0^2} e^{-\frac{j\tau}{c} \frac{\sin^2[(2N+1)\frac{\tau}{c}]}{\sin^2(\frac{\tau}{c})}}; \quad (4)$$

where  $F$  and  $F_0$  are the losses of the OPO with and without loss, respectively;  $c$  and  $\frac{c}{F}$  are the bandwidth and free spectral range (FSR) of the OPO, respectively;  $2N+1$  is the number of the longitudinal modes in the output of the OPO. The width of the peaks is  $\frac{c}{F} = (2N+1)$ , where  $\frac{c}{F} = 2 = \frac{c}{F}$  is the round-trip time of the OPO. We choose  $T$  so that  $T$  is nearly equal to  $\frac{c}{F} = 2$  but the difference between  $T$  and  $\frac{c}{F} = 2$  is longer than the width of the peaks. Then Eq.(3) can be approximated as follows:

$$\langle \rangle' = \frac{4\langle \rangle \cos^2 \frac{\tau}{c} + \langle \rangle(-T) + \langle \rangle(+T)}{16}; \quad (5)$$

$\langle \rangle'$  given by Eq.(5) is a periodic function of  $\tau$  with a period of  $\frac{c}{F}$ , which is a half of the period of classical interference. It indicates that nonclassical interference can be observed with the multimode two-photon pairs incident to the unbalanced interferometer. The physical meaning of the nonclassical interference is as follows. The multi-peaked structure of the time correlation between the multimode two photons makes it possible to distinguish the following two cases, Case1 and Case2: in Case1, both the photons are reflected or transmitted at the first beam splitter of the interferometer; in Case2, one of the two photons is reflected and the other is transmitted there. Especially in Case1, the two-photon interference is explained [10] and demonstrated [12] to be nonclassical. Thus the nonclassical phase dependence of the interference appears in Eq.(5). Furthermore, the peaks of  $\langle \rangle'$  other than the central peak induce the nonclassical interference at nonzero delay times.

As discussed in Ref.[13], the coincidence rate measured in experiments is an average of the correlation function over the resolving time,  $T_R$ , of detectors. The coincidence rate measured in this experiment will become

$$\langle \rangle = \frac{4\langle \rangle \cos^2 \frac{\tau}{c} + \langle \rangle(-T) + \langle \rangle(+T)}{16}; \quad (6)$$

where  $\langle \rangle$  is the average of  $\langle \rangle'$  (Eq.(6) in Ref.[13]).

The schematic of the experimental setup is shown in Fig.2. The differences between this setup and that used in our previous work [13] are an unbalanced interferometer between the OPO and detectors and a locking beam for the phase lock of the interferometer. The light source is a single-mode cw Ti:Sapphire laser of wavelength 860nm. The round-trip length of the OPO is

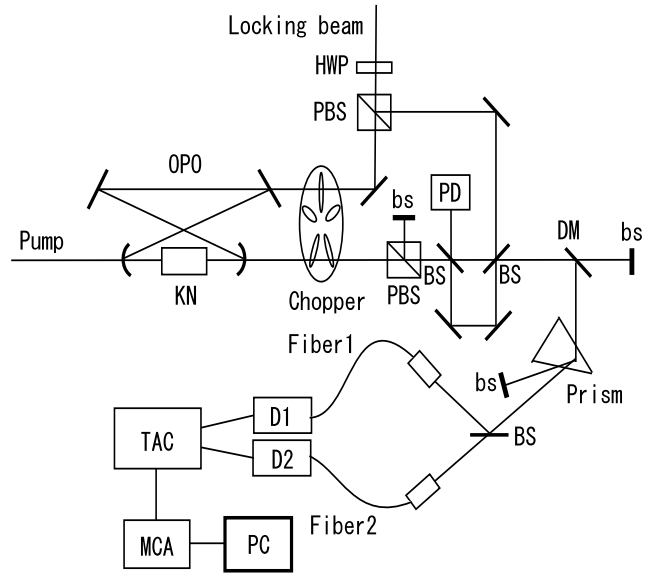


FIG. 2: Schematic of the experimental setup. PBS polarization beam splitter; HWP half wave plate; PD photodetector for phase lock; KN KNbO<sub>3</sub> crystal; DM dichroic mirror; BS 50/50 beam splitter; bs beam stop; D1 and D2 avalanche photodiodes; TAC time-to-amplitude converter; MCA multichannel analyzer.

set long (560mm) in order to time resolve the oscillatory structure in the correlation function. The output from the OPO is incident at one of the input ports of the unbalanced interferometer. The path-length difference,  $L$ , of the interferometer is set at about 29cm, which gives  $T = 0.97\text{ns}$ . Then the condition for the approximation used to derive Eq.(5) is  $2N+1 > 32$ . The phase difference of the interferometer is locked by a servo-control system. To prevent the locking beam for the interferometer from making noise, the beam propagates in the interferometer in the opposite direction to the signal beam from the OPO. Furthermore, the polarization of the locking beam is perpendicular to that of the signal in order to remove the beam by a polarization beam splitter (see Fig.2). One of the two outputs of the interferometer is split into two with a 50/50 beam splitter. The two beams are coupled to fibers and detected with avalanche photodiodes (APD, EG & G SPCM-AQR-14). The coincidence counts of the signals from the two APDs are measured with a time-to-amplitude converter (TAC, ORTEC 567) and a multichannel analyzer (MCA, NAIIG E-562). We let  $\frac{c}{F}$ ,  $T_R$ , and  $c = 2$  be 2.07ns, 280ps, and 11MHz, respectively, which were measured in Ref.[13]. We measured the coincidence counts at  $\tau = (j=8) \text{ j} (j=0; 1; \dots; 8)$ .

The experimental results at  $\tau = (j=8) \text{ j} (j=0; 1; \dots; 8)$  are shown in Fig.3-(i). The circles represent the measured coincidence counts. The lines are the fits of the data to the following equation derived from Eq.(6) [13]:

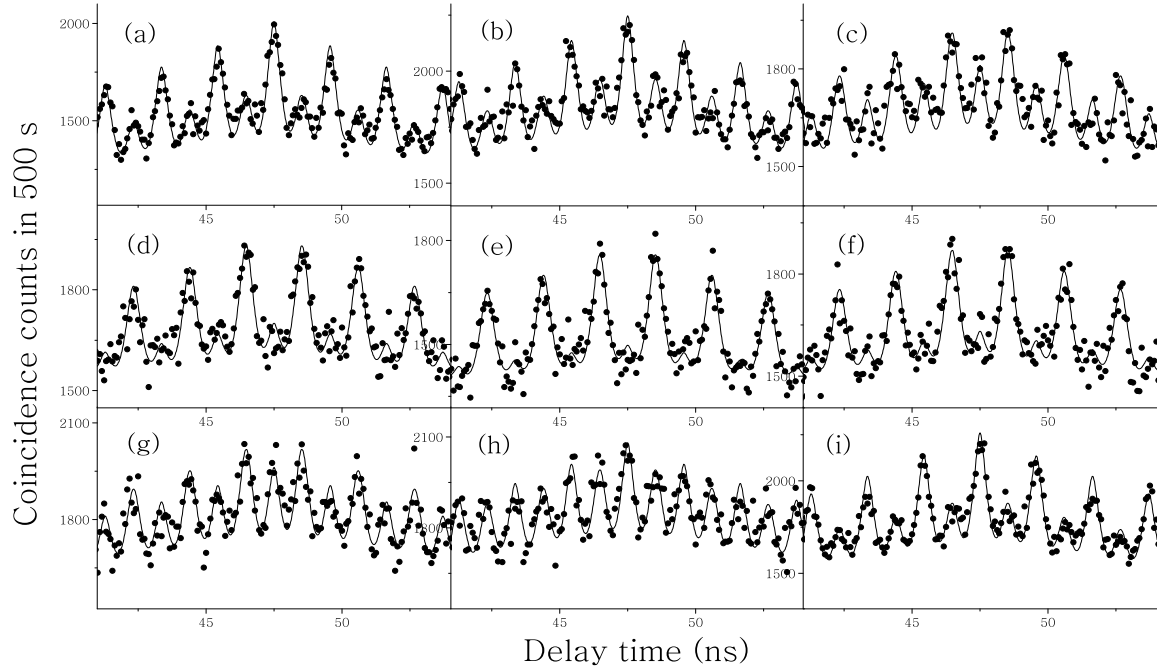


FIG. 3: Experimental results. The phase,  $\phi$ , increases stepwise by  $\pi/8$  from (a) to (i) ( $\phi = (j\pi/8)$ ;  $j = 0, 1, \dots, 8$ ). The circles represent the measured coincidence counts. The lines are the fits of the data to Eq.(7), where the fitting parameters are  $C_1$ ,  $C_2$ , and  $\phi_0$ . The fitting result of  $\phi$  is shown in Fig.4. The range of the data used for the fitting is from 18ns to 77ns.

$$c(\phi) = C_1 \frac{h}{4} \frac{(0)}{c} (\phi) \cos^2 \phi + \frac{(0)}{c} (\phi - \phi_0) + \frac{(0)}{c} (\phi + \phi_0) + C_2; \quad (7)$$

with

$$\frac{(0)}{c} (\phi) = e^{-c(j - \phi_0)X_n} \frac{1 + \frac{2j - n_F}{T_R} \frac{\phi_0 \ln 2}{\pi}}{n}; \quad (8)$$

Here the fitting parameters are two constants,  $C_1$  and  $C_2$ , and the phase difference,  $\phi_0$ ; the electric delay (zero delay time),  $\phi_0$ , is 47.5ns. The term,  $C_2$ , independent of the delay time,  $\phi$ , is mainly due to the term of higher order than  $j^2$  as discussed in our previous work [13]. The range of the data used for the fitting is from 18ns to 77ns, while the range plotted in Fig.3 is from 41ns to 54ns. We can find nonclassical interference in Fig.3 as explained below. The peaks at  $\phi = \phi_0 + n_F$  ( $n$  an integer) are higher than those at  $\phi = \phi_0 + (n + 1/2)F$  when  $n = 0$  as shown in Fig.3(a). The peaks at  $\phi = \phi_0 + n_F$  become lower as  $n$  increases from 0 to  $=2$  and reach the minimum at  $n = =2$ . After that, the peaks recover their heights as  $n$  increases from  $=2$  to  $=8$  and reach again the maximum at  $n = 8$ . The coincidence counts at  $n =$

shown in Fig.3(i) are very similar to those at  $n = 0$  shown in Fig.3(a). Therefore the period of the change of the multi-peaked correlation function is  $\pi/8$ , which is a half of that of classical interference. The phase determined from the fitting is plotted in Fig.4 against the phase locked experimentally. The inclination of the line in Fig.4 is unity. The deviations of the circles from the line are probably due to the fluctuation of the phase difference, which is shown by error bars in Fig.4, and due to an imperfect visibility, which makes the deviations around  $n = 0$ ,  $=2$ , and  $=8$  larger.

In conclusion, we have observed nonclassical interference of multimode two-photon pairs produced by an OPO with an unbalanced interferometer. The nonclassical interference has been observed at nonzero delay times. The

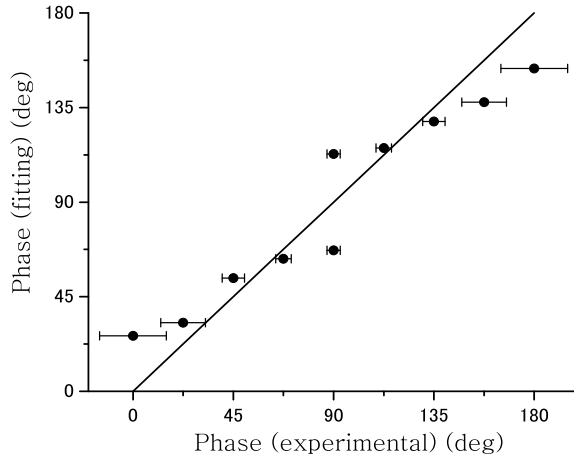


FIG. 4: Phase(fitting) determined by the fitting shown in Fig.3 is plotted against phase(experimental), which is the phase locked experimentally. The inclination of the line is unity. The error bars are estimated from the fluctuation of the phase.

observation has been explained in terms of the property of the multimode two-photon state. This is a new type of quantum interference experiment.

- [1] R. Ghosh and L. Mandel, Phys. Rev. Lett. 59, 1903 (1987)
- [2] C. K. Hong, Z. Y. Ou, and L. Mandel, Phys. Rev. Lett. 59, 2044 (1987)
- [3] Z. Y. Ou and L. Mandel, Phys. Rev. Lett. 62, 2941 (1989)
- [4] Z. Y. Ou, X. Y. Zou, L. J. Wang, and L. Mandel, Phys. Rev. A 42, 2957 (1990)
- [5] Z. Y. Ou, X. Y. Zou, L. J. Wang, and L. Mandel, Phys. Rev. Lett. 65, 321 (1990)
- [6] P. G. Kwiat, W. A. Varela, C. K. Hong, H. N. Machtel, and R. Y. Chiao, Phys. Rev. A 41, 2910 (1990)
- [7] J. G. Rarity, P. R. Tapster, E. J. Jakeman, T. Larchuk, R. A. Campos, M. C. Teich, and B. E. A. Saleh, Phys. Rev. Lett. 65, 1348 (1990)
- [8] J. B. rendel, E. M. ohler, and W. M. artienssen, Phys. Rev. Lett. 66, 1142 (1991)
- [9] Y. H. Shih, A. V. Sergienko, M. H. Rubin, T. E. Kiess, and C. O. Alley, Phys. Rev. A 49, 4243 (1994)
- [10] A. N. Boto, P. Kok, D. S. Abrams, S. L. Braunstein, C. P. Williams, and J. P. Dowling, Phys. Rev. Lett. 85, 2733 (2000)
- [11] M. D'Angelico, M. V. Chekhova, and Y. Shih, Phys. Rev. Lett. 87, 013602 (2001)
- [12] K. Edamatsu, R. Shimizu, and T. Itoh, Phys. Rev. Lett. 89, 213601 (2002)
- [13] H. Goto, Y. Yanagihara, H. Wang, T. Horikiri, and T. Kobayashi, quant-ph/0303101 (2003)
- [14] Y. J. Lu and Z. Y. Ou, Phys. Rev. A 62, 033804 (2000)